Electronic Supplementary Material (ESI) for Journal of Materials Chemistry

Supplementary Information:

In-situ synthesis of one-dimensional MWCNT/SiC porous nanocomposites with excellent microwave absorption properties

Hui-Ling Zhu, Yu-Jun Bai*, Rui Liu, Ning Lun, Yong-Xin Qi, Fu-Dong Han, Jian-Qiang Bi

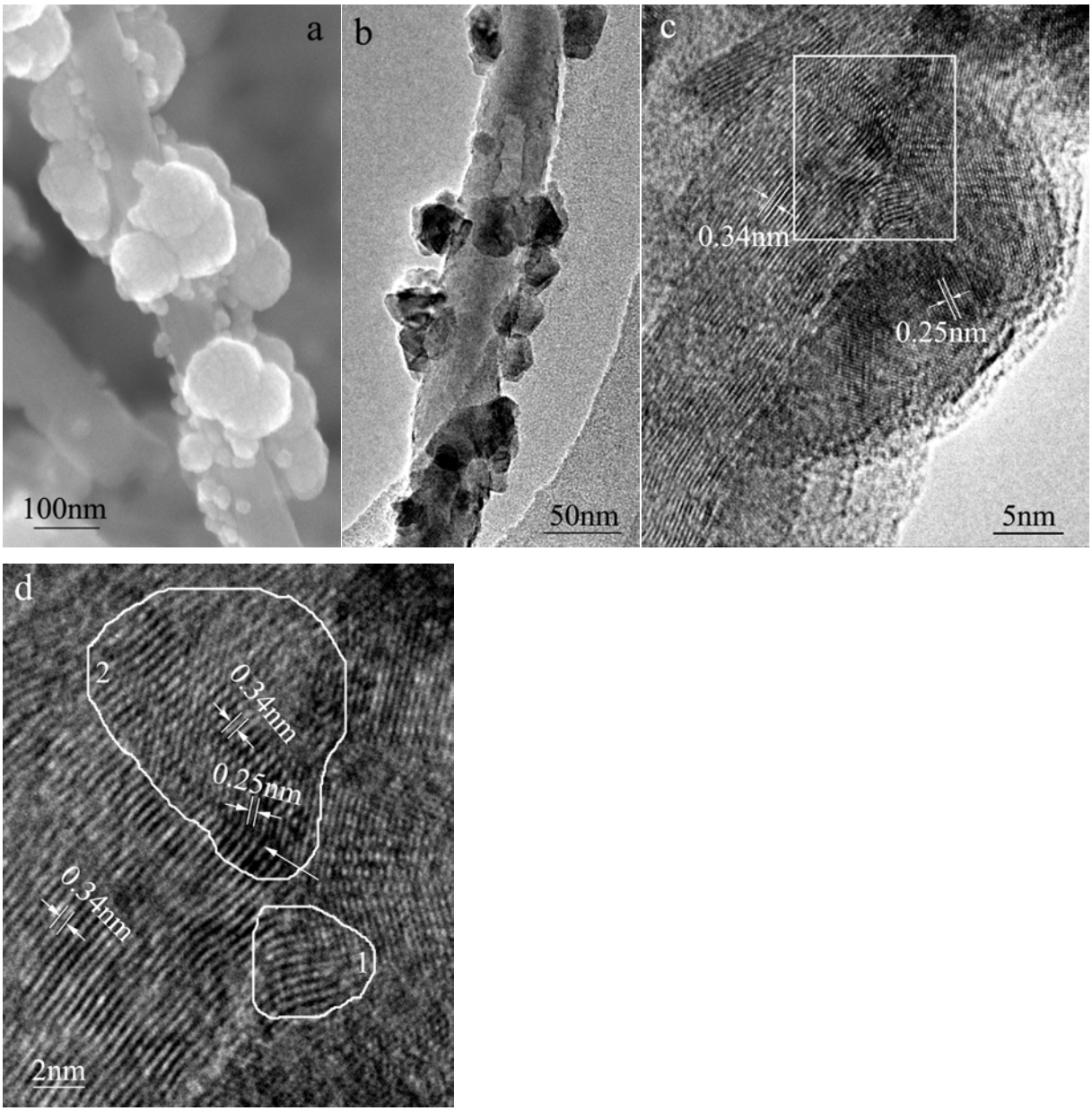

Fig. S1. FESEM (a), HRTEM (b) images of SiC nanoparticles grown along a single MWCNT and the corresponding lattice fringe images (c, d).

For further confirming the attachment of SiC nanoparticles to the MWCNTs instead of the superposition on them, more FESEM and HRTEM examinations were performed, as shown in Fig. S1. Figs. S1(a) and S1(b) clearly show the SiC nanoparticles attached to a single MWCNT, which is particularly true from the lattice fringe images (Figs. S1(c) and S1(d)). There are two different structures present on both sides of a clear interface, the lattice spacings of 0.25 and 0.34nm correspond to those of (111) plane for SiC and (002) plane for CNT, respectively. The lattice fringes of SiC are closely bonded to those of MWCNT around the interface (Fig. S1(c)). In the magnified lattice fringe image (Fig. S1(d)) acquired from the location marked with a rectangle in Fig. S1(c), the two types of lattices combine tightly. More interestingly, some transition zones can be observed between the CNT lattices and the SiC lattices, as indicated by the loops, where the lattices of CNT and SiC coexist due to the uncompleted reaction. Particularly in loop 2, the SiC lattices are growing into the CNT lattices around the thermally etched defects (marked by an arrow). As a consequence, the SiC nanoparticles indeed attach to the MWCNTs rather than simply lay over them.

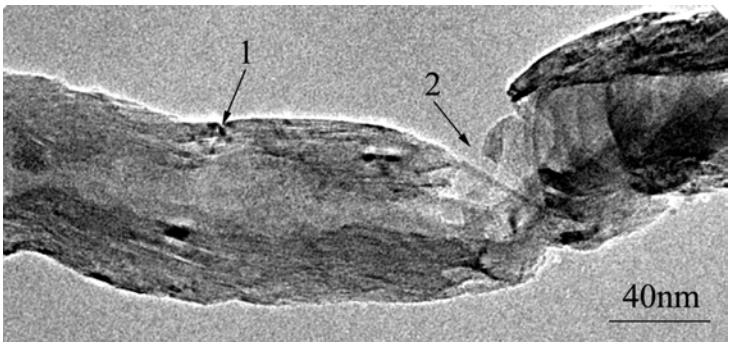

Fig. S2. A single MWCNT etched on one side observed in S400.

Fig. S2 is a TEM image observed in S400, which exhibits a single MWCNT with only one side etched. The site marked by arrow 1 indicates some representative small pores etched on

one side of the MWCNT owing to the violent thermal shock resulted from the highly exothermic reaction of Na and I_2. Meanwhile, an etching track can be observed on the opposite wall along the direction of arrow 1 because of the deficiency of heat energy. Such similar holes can also be found on the uneven surface of MWCNT shown in Fig. 1(a3). The location marked by arrow 2 displays the destruction of MWCNT at one side arising from the severe thermal shock.

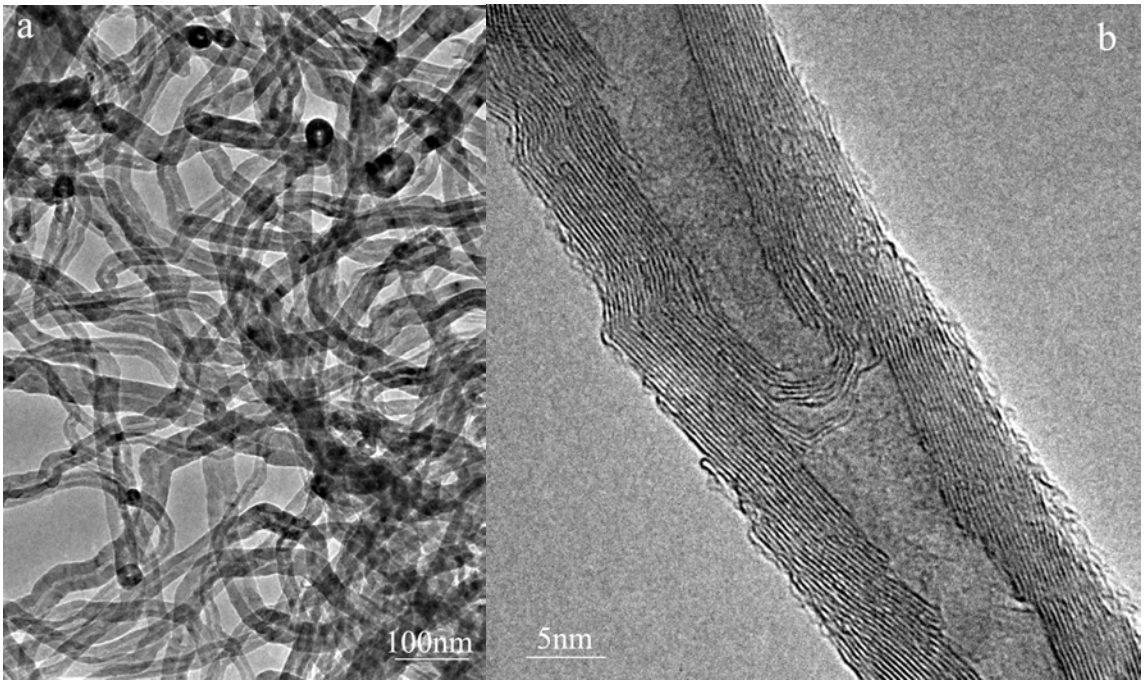

Fig. S3. TEM (a) and lattice fringe images (b) of the pristine MWCNTs used as starting material.

To verify the occurrence of thermal etching on MWCNTs during the reaction of Si, MWCNTs, Na and I_2, some direct evidences were provided. Fig. S3(a) displays the TEM images of the pristine MWCNTs before the reaction. The average diameter of the pristine MWCNTs is about 50 nm and the length is up to several micrometers. It can be seen that the surface of the pristine MWCNTs is smooth, different from those after the reaction (Fig. 1).

From Fig. S3(b), the clear lattice fringes demonstrate the high graphitization of the pristine MWCNTs, consistent with the Raman result in Fig. S4(f).

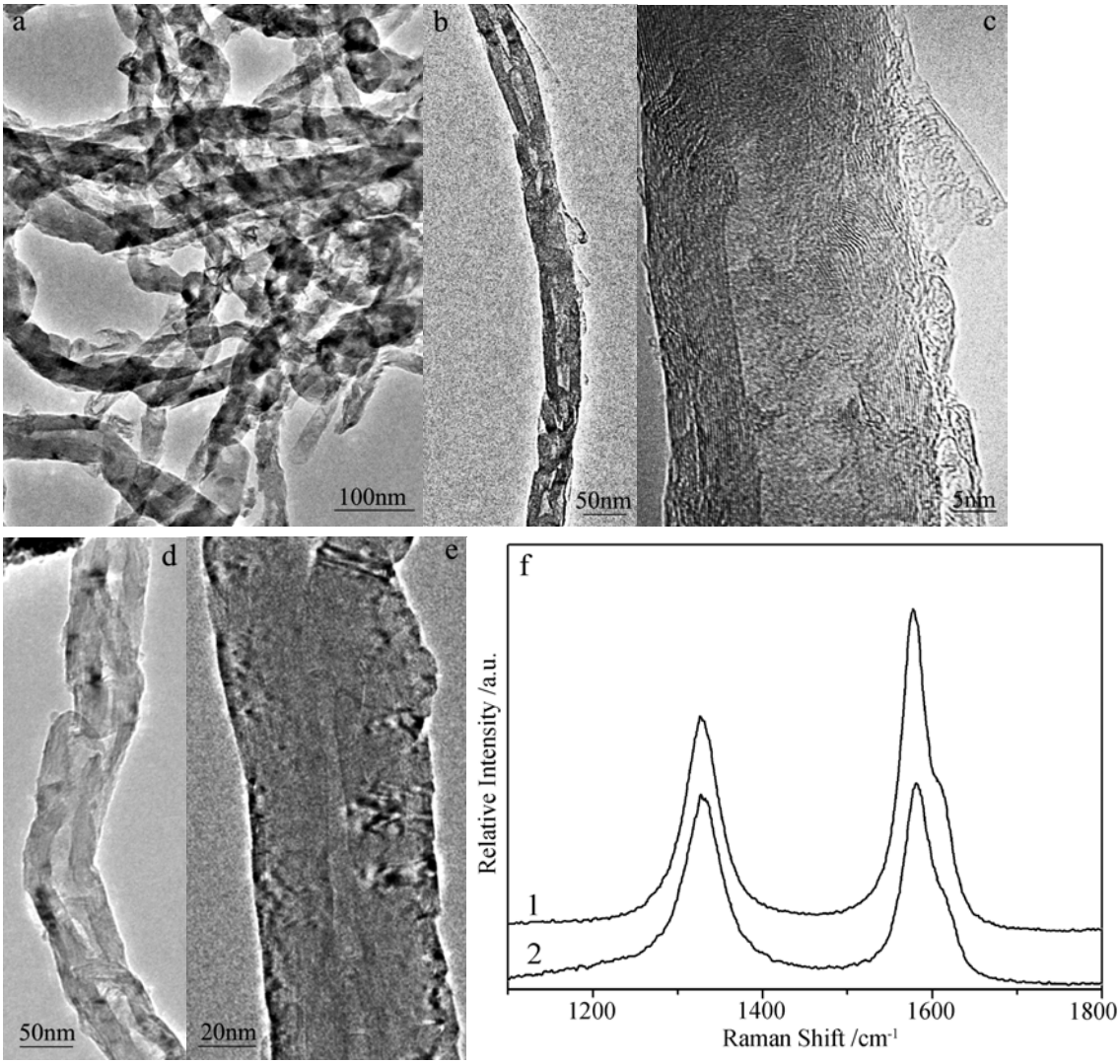

Fig. S4 TEM images (a-e) of the MWCNTs etched by the reaction of Na and I_2, and Raman spectra (f) of the pristine (curve 1) and thermally etched MWCNTs (curve 2).

For well understanding the thermal etching arising from the reaction between Na and I_2, another experiment involving MWCNTs, Na and I_2 was conducted. In a typical procedure, 1.0 g MWCNT (without further treatment), 3 g Na (cut from bulk Na) and 12.7 g I_2 powder (ground I_2 particles in an agate mortar) were put into a stainless steel autoclave with a molar

ratio of 3:5 for I_2:MWCNTs and heated to 250 °C for 1 h. The products were washed in turn with anhydrous ethanol, hydrochloric acid and distilled water, and then dried at 50 °C for 10 h. The thermal etched MWCNTs are shown in Fig. S4. It is apparent that the etched MWCNTs are greatly different from the pristine ones shown in Fig. S3. From Fig. S4(a), both the outer and inner surfaces of the MWCNTs become rough comparing with those of the pristine CNTs, and some parts of the MWCNTs become semi-transparent or transparent owing to the thermal etching on them. Fig. S4(b) displays the TEM image of a single etched MWCNT. Some graphene layers on the surface have been exfoliated locally owing to the drastic thermal shock, and some details are exhibited in Fig. S4(c). The thermally etched MWCNTs can be further confirmed by magnified TEM images shown in Figs. S4(d) and S4(e). The surface becomes accidented under the violent thermal shock with some holes occurring in the CNT, especially in Fig. S4(e), a lot of nanoholes distributing on the MWCNT could be distinctly distinguished. The structural changes of carbon materials can be effectively characterized by Raman spectroscopy. Fig. S4(f) displays the Raman spectra of the pristine MWCNTs (curve 1) and the MWCNTs etched by the reaction of Na and I_2 (curve 2). The peak around 1328 cm^{-1} (D band) is attributed to the defects and disorders in carbonaceous solid, and the peak centered at 1577 cm^{-1} (G band) is due to the stretching modes of C-C bonds of typical graphite. The intensity ratio of I_D/I_G can be regarded as a usual measurement for the graphitic ordering, the greater the ratio of I_D/I_G, the higher the disorder degree for graphite. The calculated I_D/I_G value is about 0.67 for the pristine MWCNTs and 0.95 for the etched MWCNTs, demonstrating that the etched MWCNTs exhibit low graphitization degree with more defects, in good agreement with the TEM images shown in Figs. S3 and S4 (a-e). The Raman spectra

further verify the structural changes and defects in the MWCNTs arising from the reaction of Na and I_2.